The Cryosphere Discuss., 4, 1931–1966, 2010
www.the-cryosphere-discuss.net/4/1931/2010/
doi:10.5194/tcd-4-1931-2010

The Cryosphere Discussions

Landsat TM and ETM+ derived snowline altitudes in the Cordillera Huayhuash and Cordillera Raura, Peru, 1986–2005

E. M. McFadden[1,2], **J. Ramage**[1], **and D. T. Rodbell**[3]

[1]Earth and Environmental Sciences, Lehigh University, 1 West Packer Ave., Bethlehem, PA 18015, USA
[2]Byrd Polar Research Center, The Ohio State University, 1090 Carmack Road, Columbus, OH, 43210, USA
[3]Geology Dept., Union College, Schenectady, NY 12308, USA

Received: 13 August 2010 – Accepted: 24 August 2010 – Published: 6 October 2010

Correspondence to: J. Ramage (ramage@lehigh.edu)

Published by Copernicus Publications on behalf of the European Geosciences Union.

Abstract

The Cordilleras Huayhuash and Raura are remote glacierized ranges in the Andes Mountains of Peru. A robust assessment of modern glacier change is important for understanding how regional change affects Andean communities, and for placing paleoglaciers in a context relative to modern glaciation and climate. Snowline altitudes (SLAs) derived from satellite imagery are used as a proxy for modern (1986–2005) local climate change in a key transition zone in the Andes.

Clear sky, dry season Landsat Thematic Mapper (TM) and Enhanced Thematic Mapper (ETM+) satellite images from 1986–2005 were used to identify snowline positions, and their altitude ranges were extracted from an Advanced Spaceborne Thermal Emission and Reflection Radiometer (ASTER) DEM. Based on satellite records from 31 glaciers, mean snowline altitudes (SLAs), an approximation for the equilibrium line altitudes (ELAs), for the Cordillera Huayhuash (13 glaciers) and Cordillera Raura (18 glaciers) were 5046 m a.s.l. and 5013 m a.s.l., respectively, from 1986–2005. The rate of SLA rise was 25 m/decade in the Cordillera Huayhuash and 62 m/decade in the Cordillera Raura.

1 Introduction

The Cordilleras Huayhuash (10°15′ S, 76°55′ W) and Raura (10°27′ S, 76°46′ W) are tropical glacierized ranges located in a remote region of the Andes Mountains in central Peru (inset of Fig. 1). The Cordillera Huayhuash is southeast of the larger and better known Cordillera Blanca, and has 117 glaciers covering ~85 km^2 (Morales Arnao, 2001). Peaks are typically over 6000 m a.s.l. with the highest peak recorded at 6617 m a.s.l. (Nevado Yerupajá). The Cordillera Raura, located to the southeast of the Cordillera Huayhuash, has a slightly smaller (55 km^2) glacier area (Morales Arnao, 2001). The close proximity of the two ranges allows for a reasonable comparison of snowline altitude (SLA) change and assessment of potential regional causes of SLA

TCD
4, 1931–1966, 2010

change. The climate on the eastern side of the Andes is largely affected by orographic uplift and condensation of moist tropical air from the Amazon basin creating an east-west precipitation decrease (Kaser and Osmaston, 2002). Modern Tropical Rainfall Mapping Mission- (TRMM) derived precipitation highlighting the east to west gradients are shown effectively at a >5 km scale in Bookhagen and Strecker (2008).

In this study, remote sensing was employed to measure and map modern snowlines (snow-ice boundaries), as an approximation of the equilibrium line altitude (ELA). Snowlines at the end of the melt season map the minimum elevation where glacial ice is continuously covered by snow. Snowlines serve as a good proxy for ELA and therefore for mass balance and climate reconstructions. Snowlines in this tropical environment generally track ELAs although they can be slightly lower than the ELA (Andrews, 1975; Klein and Isacks, 1998). A snowline mapped during the dry season when snow cover is at an annual minimum approximates the corresponding annual ELA position in areas without superimposed ice (Klein and Isacks, 1998). Remote sensing allows spatially consistent temporal reconstruction of SLAs over the past twenty years in this high relief region. In order to accurately measure SLAs in the Cordilleras Huayhuash and Raura, satellite imagery was analyzed based on the unique reflectance characteristics of different materials at visible and near infrared wavelengths.

Although both snowlines and terminus positions are easily measured using remote sensing, snowlines were monitored here because they respond directly and annually to local climate variability. This 20-year record of modern SLA variability is important for predicting future rates of change. Modern SLA variability is also important on a local scale, as the glaciers are important sources of water for agriculture, hydroelectric power, and consumption, particularly during the dry season (Kaser et al., 2003; Mark, 2005; Bradley et al., 2006). SLA variability is used as a proxy for climate change in a region where climate data are scarce yet important on both local and global scales. Our data portray interesting temporal and spatial variations in SLAs throughout the study region.

TCD
4, 1931–1966, 2010

2 Methods

2.1 Satellite image selection

Landsat 5 Thematic Mapper (TM) and Landsat 7 Enhanced Thematic Mapper (ETM+) data with 28.5-meter resolution were used for snowline observations. Landsat 5 TM data were compiled for 1986, 1989, 1991, 1996, and 1997 and Landsat 7 ETM+ data were used compiled for 1999, 2002, 2004, and 2005. Dates and sources for each image are in Table 1.

Images were preferentially selected during the dry season to maximize the probability of extracting snowlines at minimum snow-cover. One December (wet season) image was included from 1989 to fill the gap in the late 1980s, and it displays the lowest snowlines of any measured. In this region of Peru, the dry season begins during May and gradually ends through September with typically only 20% of the total annual precipitation recorded over this time (Schwerdtfeger, 1976). Seven of nine images were taken from June through August to best approximate minimum snow cover (Table 1). Although the images are not from the same date, they are the best Landsat images available for SLA approximation by snowline measurement. Images with signs of recent high elevation snowfall were not included because they represent a short-term SLA adjustment rather than the dry season snowline. Absence of cloud cover was also considered because clouds obscure glaciers and create shadows that complicate the classification process. The high relief of the ranges also means that many small glaciers could not be included due to the presence of shadows. These constraints limited snowline measurement to 9 years over a twenty year period on 31 glaciers in the Cordilleras Huayhuash and Raura.

Glacierized valleys are identified using the name of the lake in the closest valley (Fig. 2; A-Z and AA-EE). Since cocha means lake in Quechua, most valleys contain cocha in part of their name. This naming scheme is used whenever possible for glaciers to minimize confusion. If a lake was not located within a reasonable distance from the glacial terminus, then the nearest peak was used.

TCD
4, 1931–1966, 2010

2.2 Image calibration

Landsat 5 TM data used for SLA measurements were calibrated to radiance and then planetary reflectance as a method of standardization. Similar calibration techniques were employed on Bolivian Landsat TM images by Klein and Isacks (1998) to improve the quality of snow-ice differentiation. The procedures for calibration employed in this study were taken from Chander and Markham (2003). Once calibrated for radiance and reflectance, images had pixel values ranging from 0–1.0, representing planetary surface reflectance as a ratio. The equations used for all calibrations are found below (Eqs. 1 and 2). Data from Tables 1, 2, and 3 were used in these calculations.

The following procedures were used to calibrate images according to the effects of different solar angles and irradiance values between bands. To calibrate the images, metadata were provided by the Global Land Cover Facility (GLCF) at the University of Maryland, or by the United States Geological Society, EROS Data Center (EDC) (Table 1).

Radiance was calculated as:

$$L_\lambda = \left[(L_{\max} - L_{\min})\mathrm{DN}_{\max}^{-1}\right] * \mathrm{DN} + L_{\min} \quad (1)$$

The variables were defined by:
L_λ = spectral radiance in $\mathrm{Wm}^{-2}\mathrm{sr}^{-1}\mu\mathrm{m}^{-1}$
$L_{\min}$ = spectral radiance where DN = 0; (Table 2)
$L_{\max}$ = spectral radiance where DN = 255; (Table 2)
DN = the value of each wavelength band from Landsat 5 TM data (1,2,3,4,5,7)
$\mathrm{DN}_{\max}$ = maximum value for each band.

Bands were corrected individually to account for unique $\mathrm{DN}_{\max}$ values and the wavelength specific data found in Table 2. Values from Table 2 can be used for Landsat 5 TM images taken between 1 March, 1984 and 4 May, 2003 (Chander and Markham, 2003).

TCD
4, 1931–1966, 2010

Equation 2 was used in conjunction with the radiance images to create an image directly comparable to pre-calibrated Landsat 7 ETM+ images. Planetary reflectance was calculated from:

$$\rho_P = \pi L_\lambda d^2 S^{-1} \mu^{-1} \quad (2)$$

where,
ρ_P = wavelength-specific planetary reflectance (dimensionless)
d = Earth–Sun distance (astronomical units) (Table 1)
S = band-specific solar exoatmospheric irradiance ($Wm^{-2}\,\mu m^{-1}$)
μ = cosine of the solar zenith angle.

Earth-Sun distances were obtained based on the day of year when each image was taken. The solar zenith angle (SZA) is $\pi/2$ – solar elevation (radians). This process eliminates the effects of the changing position of the sun between images. Once all variables were defined, each band was calibrated to planetary reflectance (ρ_p) using the data for solar exoatmospheric irradiance (S) from Table 3 and Eq. 2 (Chander and Markham, 2003).

2.3 Geographic registration

After completing calibration, the images were geographically registered to the coordinate system from the previously georeferenced 1997 ETM+ image. The coordinate system (UTM 18S, WGS 84 datum) from the 1997 image was selected as the base because the image displays the largest glaciated area including the Cordilleras Blanca, Huayhuash, and Raura. A large number (>80) of ground control points (GCPs) distributed throughout each image were selected for georeferencing purposes. GCPs were focused around, but did not include, glacial margins due to their annual variability. All other images were georeferenced using GCPs and registered to the 1997 image. Some coordinate offsets of ± 140 m (± 5 pixels) magnitude are present in several registered images but the offsets are confined to the highest peaks where distortion is

TCD
4, 1931–1966, 2010

expected as these images were registered, not orthorectified. There is little distortion in the SLA zones.

2.4 Supervised classification

We used supervised classification of each calibrated image to get the snow-ice boundary. This method was used rather than the standard TM bands 4/5 ratio method applied by De Angelis et al. (2007) because calibrated images had enough variability in the spectral values of various materials that some features were clearly misclassified. Each image was classified individually to prevent false classification of snow and ice due to overlapping pixel ranges. Training areas such as clear water, snow, ice, clouds, snow in shadow, recently exposed bedrock, weathered bedrock, wetlands, slopes with vegetation, and water containing glacial flour were defined on each image to incorporate various materials necessary for characterizing the image and distinguishing snow and ice. Training area size and material composition were selected to minimize user bias and image variations. Each training area, composed of multiple individual regions, contained over one hundred pixels. Borderline pixels were excluded from training area differentiation to prevent overlapping values and false classification. Avalanche-fed glaciers were also avoided during training area classification due to ambiguous pixel coloration. Images were classified based on their training area pixel values in order to create an image with all materials distinguished by their spectral values rather than manual interpretation.

2.5 DEM comparison and snowline elevation extraction

Linear overlays representing snowlines were created following image classification. The snowlines were overlaid on two digital elevation models (DEMs) to extract SLAs. DEMs were from the Shuttle Radar Topography Mission (SRTM) and the Advanced Spaceborne Thermal Emission and Reflection Radiometer (ASTER). The SRTM and ASTER DEMs were compared using identifiable ground features (e.g. moraines) to determine their accuracy.

TCD
4, 1931–1966, 2010

The SRTM DEM was collected in February 2000, to provide near global 3-arc second (90-m) elevation data. Significant data gaps exist from shadow and layover in high relief areas due to the synthetic aperture radar geometry. Data gaps were patched with over-sampled GTOPO 30 data with 30-arc second (1 km) resolution (Bliss and Olsen, 1996). The patched resolution was still inadequate, as high resolution was necessary for SLA measurements in several patched areas. To improve the problem of extracting reliable elevations, the stereo capabilities of ASTER band 3N (nadir) and 3B (backward) allowed creation of a DEM with 15-m spatial resolution using the ASTER_DTM module for ENVI (Fig. 1). The ASTER Image was from 30 June, 2004. ASTER data are higher resolution, but peak elevations were inaccurate. Despite the coarse elevations provided by the lower resolution SRTM DEM, it was used with La Carta Nacional 1:100,000 topographic map (Yanahuanca: Hoja 21-j) of Peru to determine the extent of the ASTER DEM limitations. Elevations were compared at multiple locations (>100), exposing a region of underestimated elevations above 5600 m on the ASTER DEM relative to both the SRTM DEM and the topographic map. Because SLAs were below the inaccurate region, the ASTER DEM was considered the most accurate DEM for SLA extraction. Error analysis from the comparison between the two DEMs is beyond the scope of this paper and can be summarized as the ASTER DEM is reliable below 5600 m a.s.l. and less reliable at elevations greater than 5600 m a.s.l.

Linear overlays representing snowlines were mapped for each of 31 glaciers for every year with useable imagery and overlaid onto the ASTER DEM to determine the altitude range of snowlines (Fig. 2, Tables 4 and 5). ASTER DEM elevations were extracted from all cells intersecting the linear overlays, providing minimum, maximum, mean, and standard deviation values for the annual snowline on each glacier. Tables 4 and 5 show the mean and standard deviation for each glacier's snowlines for the Cordillera Huayhuash and the Cordillera Raura respectively. Snowlines are used to approximate the glacier ELAs. Values discussed throughout the text are the mean value that may have a wide variation across the glacier.

TCD
4, 1931–1966, 2010

3 Results

Overall, snowlines were calculated for 31 glaciers: 13 glaciers in the Cordillera Huayhuash and 18 glaciers in the Cordillera Raura. In the Cordillera Huayhuash, individual glacier snowlines range from 4823 ± 31 m a.s.l. (Quesillococha (F) 1986) to 5474 ± 44 m a.s.l. (Rasac (M) 2002), a range of 651 m. The mean snowline over the 20 year period for the Cordillera Huayhuash ranges from 5008 ± 54 m a.s.l. to 5086 ± 35 m a.s.l. Individual glaciers in the Cordillera Raura have a snowline range from 4743 ± 5 m a.s.l. (Viconga (V) 1986) to 5196 ± 59 m a.s.l. (Pichuycocha (AA) 2002), a range of 453 m. The mean snowline over the 20 year period for the Cordillera Raura ranges from a minimum of 4947 ± 7 m a.s.l. to a maximum of 5070 ± 17 m a.s.l.

During the study period from 1986 to 2005, glaciers in the Cordillera Huayhuash showed much greater variability in snowline elevation than those in the Cordillera Raura. We looked at the annual snowlines for each glacier, the mean for the range, and the 20-year trends both individually and combined. Individual snowlines are shown in Table 4, Table 5, and Fig. 2. Trends were compared across ranges and throughout time in an effort to explain spatial variability for both the snowline and the year-to-year change in snowline altitude (ΔSLA) (Figs. 5, 6, 7).

The standard deviations for the mean snowline for the Cordillera Huayhuash are larger than those for the Cordillera Raura due to the of several glaciers with widths >1-km in the Cordillera Huayhuash. These glaciers the mean snowline standard deviation, calculated as the square root of the sum of the variances for the individual glaciers divided by the number of glaciers included in the mean. For the purpose of the statistical calculations used to derive the mean snowlines and standard deviations, snowlines for each glacier are assumed to be independent. In order to determine statistical significance of snowline differences, a normal distribution was assumed for all snowlines. Although this assumption may be invalid when sample size is quite small ($n < 5$), the assumption is necessary to perform the 2-sample t-tests used in this study.

TCD
4, 1931–1966, 2010

3.1 Glaciers of the Cordillera Huayhuash

The mean snowline for the Cordillera Huayhuash was used to obtain a better understanding of the overall change in snowlines in comparison with individually analyzed glacial trends. Due to absence of data from the Rasac (M) glacier in most years and its abnormally high snowlines, it was excluded from the calculation of the mean snowline for the Cordillera Huayhuash throughout the study period. If included, the mean snowline altitude rose by nearly 30 m for the two recorded years with Rasac data. To examine the validity of the calculated average for the entire Cordillera Huayhuash, it was compared to snowline altitudes from the Mitococha (B) and Quesillococha (F) glaciers located within the range. These glaciers were also used in comparison with the average snowline altitudes for the Cordillera Huayhuash to highlight the variety of individual trends throughout the time series.

The colored lines in Fig. 2 display the snowlines for each available year as vector overlays on the 1997 Landsat TM band-3 base image. To examine SLA trends throughout the Cordillera Huayhuash, each glacier's SLAs were also compared to the mean SLA for the range. Overall, the mean SLA for the Cordillera Huayhuash rose from 5062 ± 36 m a.s.l. in 1986 to 5086 ± 35 m a.s.l. in 2005. Although the SLA rise is not statistically significant at the 95% confidence level ($P = 0.076$), the relatively small P-value indicates that the rise is fairly unlikely to be a product of random natural variability alone.

Analysis of the mean and individual SLAs indicates that some of the thirteen glaciers in the Cordillera Huayhuash provide more reliable SLAs than others; calculated SLAs are most reliable in valleys that are not avalanche-fed and where SLAs can be measured in almost all Landsat images throughout the time series. The Sarapococha (K) and Rasac (M) glaciers may be unreliable due to shadow obscuring their snowline in several images and the Gangrajanca (E) glacier was considered unreliable for several years due to recent avalanches. All 13 glaciers with long-term records were compared to create a comprehensive mean SLA and to analyze the spatial distribution of modern SLA change throughout the Cordillera Huayhuash.

TCD
4, 1931–1966, 2010

The general SLA rise in the Cordillera Huayhuash is exemplified by the Quesillococha (F) glacier (Fig. 3), which shows rising SLAs in the last 20 years. The eastward-facing Quesillococha (F) glacier is located near Yerupajá on the eastern side of the Cordillera Huayhuash. Between 1986 and 2005, the Quesillococha SLA rose from 4875 ± 40 m a.s.l. to 4991 ± 40 m a.s.l. and in plan view moved headward (west) by ~116 m. Overall, the SLA rose over 100 m in nineteen years (Fig. 3).

SLA and ΔSLA variations from glacier to glacier reflect unique accumulation and ablation conditions of individual valleys. The plots displayed in Fig. 4 display the temporal trends for the mean SLAs of all glaciers in the Cordillera Huayhuash and the Cordillera Raura. The error bars are plus-or-minus one standard deviation from the mean. Plots of the Cordillera Huayhuash SLAs are arranged alphabetically according to the glacier IDs (Fig. 2 and Table 4), as are those of the Cordillera Raura (Fig. 2 and Table 5).

We compare the average SLAs to Jahuacocha (A) and Chaclan (C) glaciers (10°14.5′ S) in the Cordillera Huayhuash. The Jahuacocha glacier had the most dynamic annual variation and SLAs higher than the mean from 1986 to 2005. The Chaclan glacier is on the opposite side of the ridge at similar latitude making it a reasonable glacier for comparative purposes. From 1986 to 2005, the Jahuacocha SLAs rose from 5272 ± 117 m a.s.l. to 5291 ± 117 m a.s.l. The Chaclan SLA rose comparably (~30 m) between 1996 and 1997 alone, with a similar rise occurring on 3 other glaciers over the same year. During this time period the Jahuacocha SLA fell by ~96 m. Though the changes in SLA have no obvious spatial pattern (Figs. 5, 6), they demonstrate the rapid response of snowline positions to temperature change on annual scales. Also, the large annual changes in the position of the Jahuacocha SLA demonstrate the need to examine overall SLA trends rather than annual trends alone.

Consistency of individual SLAs lower than or higher than the mean for the range is another important aspect of the Cordillera Huayhuash data set. Almost all measurable glaciers have SLAs either entirely lower than or higher than the mean throughout the time series with little annual cross-over. The glaciers with SLAs lower than the mean for nearly every year are Mitococha (B), Chaclan (C), Quesillococha (F), Carnicero

TCD
4, 1931–1966, 2010

(H), Barrosacocha (I), and Jurau (J) shown with red labels in Fig. 2. All other SLAs are nearly always.

Klein and Isacks (1998) mapped a strong east-west SLA difference from 1984 to 1987 across the eastern ridge of the Andes Mountains in southern Peru using remote sensing techniques similar to those described above. Although their data describe the eastern branch of the Cordillera, the trend of lower eastern and higher western snowlines should exist in the Cordillera Huayhuash as well due to similar easterly sources of precipitation (e.g Kaser and Osmaston, 2002; Bookhagen and Strecker, 2008). Although lower SLAs were expected along the eastern side of the ridge in the Cordillera Huayhuash, only half of the glaciers on the eastern side had SLAs lower than the mean during the study period. It is not easy to explain the pattern, though there are two distinct groups are evident. One of the groups is in the northeast part of the range and the other is in the southern part of the range spanning the east and west sides of the ridge (Fig. 2). One possibility is that different valley orientations with respect to high mountain peaks may channel moist air into the lower SLA valleys and deflect moist air from the higher SLA valleys. Although this theory would explain the lower SLA trends, the exact mechanisms causing the air movement are not clear.

Spatial and temporal trends in the Cordillera Huayhuash are shown in Fig. 5. Although Fig. 5 displays individual glacier SLA trends throughout the time series, broad elevation zones (100 m) obscure small SLA changes. Therefore, these spatial representations are best used to assess annual spatial variability in relative snowline positions between glaciers rather than temporal changes of individual glaciers.

Figure 6a displays the spatial distribution of snowline change from 1986 to 2005 in the Cordillera Huayhuash. All glaciers with falling SLAs from 1986 to 2005 are located on the eastern side of the range. These four glaciers are the Chaclan (C), Carhuacocha (D), Gangrajanca (E), and Azulcocha (G) glaciers. Two glaciers with significant SLA rises are also found on the eastern side of the range.

TCD
4, 1931–1966, 2010

The glaciers with rising SLAs on the eastern side of the Cordillera Huayhaush are the Quesillococha (F) and Carnicero (H) glaciers. SLAs for both glaciers rose more than 70 m during the study period. The large rise generates questions regarding why these glaciers are so different from nearby glaciers. We investigated the possibility of unreliable images to determine the validity of all measurements. Abnormally low SLAs could be attributed to recent high elevation snow events, creating a larger SLA rise overall. We all images with recent snowfall on the glaciers, minimizing the aforementioned effects on measured SLAs.

3.2 Glaciers of the Cordillera Raura

The Cordillera Raura SLAs provide a helpful comparison with the Cordillera Huayhuash SLAs because the close proximity of the ranges. Eighteen glaciers in the Cordillera Raura were observed from 1986 to 2005 with satellite images from 6 years during the study period.

The mean SLA for the Cordillera Raura rose from 4947 ± 7 m a.s.l. to 5070 ± 17 m a.s.l. from 1986 to 2005. The mean SLA rise is statistically significant at the 95% confidence level ($P = 0.000$), indicating that the SLA rise is large enough that we can confidently say it reflects real SLA change rather than random variability. Although data were more limited for the Cordillera Raura (6 dates over 20 years), the time series provided a fairly consistent data set for individual glaciers. The most important temporal trend derived from the Cordillera Raura was the rising SLAs on all glaciers throughout the range (Fig. 4). Individual glacier ΔSLAs ranged from negligible change on the Caballeros (Y) glacier to +236 m on the Yuracocha (T) glacier. Although there is a great deal of variability in ΔSLA values throughout the range, the mean ΔSLA was +123 m.

Spatial variability throughout the Cordillera Raura demonstrates an east-west contrast in SLA trends that differs from the Cordillera Huayhuash. Spatial variability is displayed in a time series for the Cordillera Raura (Figs. 6, 7), providing general SLA spatial variability and trends from 1986 to 2005. On average, SLAs from glaciers on the

TCD
4, 1931–1966, 2010

western side of the ridge have lower SLAs than those on the eastern side; in contrast to the Cordillera Huayhuash which had lower SLAs on the eastern side of the ridge. The east-west difference, largest in 1986, decreased in magnitude during the study period due to a more rapid SLA rise on the western side of the ridge. In 1986, the western SLAs (Fig. 2) were located at at a mean elevation of 4878 ± 10 m a.s.l. and eastern SLAs were located at a mean of 5008 ± 9 m a.s.l. In 2002, the SLAs were located at mean elevations of 5031 ± 9 m a.s.l. and 5055 ± 11 m a.s.l. respectively. The difference between the eastern and western SLAs is statistically significant at the 95% confidence level for 1986 ($P = 0.000$) and for 2002 ($P = 0.000$). The results of the t-test suggest that although the difference between eastern and western SLAs is decreasing with time, the difference has not become small enough to be attributed to random variability alone. A t-test could not be performed for 2005 because data were only available for the glaciers on the west side of the ridge.

A simple comparison of SLA trends between the Cordillera Huayhuash and the Cordillera Raura displays multiple similarities as well as noticeable differences between the two ranges. Although the ranges are located in close proximity, their mean SLA trends are quite different. As shown in Figs. 6 and 8, the SLAs from 1986 are much lower in the Cordillera Raura (4947 m) than the Cordillera Huayhuash (5062 m). However, the SLAs in the Cordillera Raura showed a more steady, significant rise from 1986 to 2005 than the Cordillera Huayhuash, resulting in comparable SLA values in 2005. In 2005, the Cordillera Raura had a mean SLA of 5070 ± 17 m a.s.l. and the Cordillera Huayhuash had a mean SLA of 5086 ± 35 m a.s.l.

Other interesting spatial trends arise when comparing the two ranges. Overall, the SLAs on the eastern side of the ridge are lower than the mean SLA in the Cordillera Huayhuash but higher than the mean SLA in the Cordillera Raura. However, eastern SLAs in both ranges rise at a slower rate than their respective western SLAs. Furthermore, the SLAs in the Cordillera Huayhuash are rising at a slower rate on average than those in the Cordillera Raura. Fig. 6a, b display the SLA changes from 1986 to 2005 for individual glaciers throughout both ranges. This figure visually demonstrates

TCD
4, 1931–1966, 2010

the east-west differences in both ranges as well as the more rapidly rising SLAs in the Cordillera Raura (+123 m) compared to the Cordillera Huayhuash (+25 m) from 1986 to 2005. Similar east-west differences have been noted in the Cordillera Blanca by Kaser et al. (1996) and Kaser and Georges (1997) which can only be partly accounted for by temperature change throughout the region. Kaser et al. (1996) concluded that the variability is only half-explained by temperature change and Kaser and Georges (1997) state that humidity, precipitation, and cloud cover are more important variables affecting SLA position. Therefore, for future SLA change, it is not known whether the trends will continue to converge or continue at different rates based on a large number of variables.

4 Discussion and conclusions

SLAs in the Cordilleras Huayhuash and Raura are temporally and spatially variable. From 1986 to 2005, the mean SLA in the Cordillera Huayhuash rose from 5062 ± 36 m a.s.l. to 5086 ± 35 m a.s.l. In the Cordillera Raura, the mean SLA rose from 4947 ± 7 m a.s.l. to 5070 ± 17 m a.s.l. over the same time period. Modern SLAs in southern Peru have been documented near 5200 m (Mark et al., 2002; Dornbusch, 1998), and the lower SLAs documented here may be attributed to topographic and/or climatic differences between the regions. Although most moisture from the air condenses and falls on the eastern side of the range before crossing the high peaks, increased precipitation from the Amazon basin would affect SLAs throughout the range.

Mean SLAs are indicative of the general trends throughout each range, however, they do not adequately represent the full variation of SLAs on the east and west sides of the Cordilleras Huayhuash and Raura. In general, glaciers on the western side of the divide had distinctly higher SLAs than those on the eastern side in the Cordillera Huayhuash with the opposite trend (lower SLAs on the western side of the ridge) displayed across the Cordillera Raura (Fig. 7). Mean SLAs were 5050 ± 19 m a.s.l. and 5100 ± 148 m a.s.l. in 1986 and 5015 ± 19 m a.s.l. and 5069 ± 57 m a.s.l. in 2002 for the

TCD
4, 1931–1966, 2010

eastern and western sides respectively. The difference across the ridge was not statistically significant in 1986 ($P = 0.358$) or in 2002 ($P = 0.082$), most likely because of the large standard deviation of the mean SLA on the western side of the ridge. Similarly, the difference across the ridge was not statistically significant in 2005 ($P = 0.183$) when the mean SLAs for the eastern and western sides were 5069 ± 11 m a.s.l. and 5116 ± 88 m a.s.l. respectively. The lack of statistical significance in the difference between the eastern and western SLAs is most likely from the large western standard deviation from the influence of the >100 m standard deviation of Jurau (J) glacier (Fig. 4) and the relatively small difference (~50 m) across the ridge.

Despite the lack of statistical significance in the difference across the ridge, the lower SLAs on the eastern side of the ridge in the Cordillera Huayhuash may indicate different climate conditions across the crest of this range. Lower SLAs on the eastern side of the ridge are caused by increased moisture and precipitation from the adiabatic cooling of moist air from the Amazon basin as it rises over the high mountain peaks. Although temperature differences significantly change SLA position over time, temperature differences across the ridge have minimal effects on the east-west climate variability relative to the moisture gradient. The opposite pattern in the Cordillera Raura is not as easily explained since moist Amazon air should also contribute to lower SLAs on the eastern side of the ridge. The presence of lower SLAs on the western side of the ridge indicates multiple controls of SLA position such as valley orientation, microclimate, hypsometry, and catchment area.

Although moisture differences across the ridge may cause east-west SLA variability, mean SLAs are used to represent the prevalent trends in the Cordilleras Huayhuash and Raura because should be reduced when calculating the mean. Therefore, a rise in the mean SLAs for both ranges indicates a shift toward a warmer and possibly drier climate in the central Peruvian Andes. In general, SLA change is best explained by either decreased accumulation in the wet season or increased ablation during the dry season, or both factors combined. However, in general, annual precipitation changes have little effect on SLAs in the inner tropics relative to variations in air temperature

TCD
4, 1931–1966, 2010

(Francou et al., 2004; Kaser and Osmaston, 2002). Since the dispersion coefficient indicating annual variations in precipitation is 14% in the Peruvian Andes (Schwerdtfeger, 1976), suggesting (on average) little precipitation change over the 20 year study, moisture variation is not likely the primary cause of short-term SLA variability. Furthermore, temperature in the tropical Andes is strongly correlated to humidity, cloudiness, and precipitation (Vuille et al., 2008) indicating that temperature variation is an extremely important factor regarding SLA change.

Therefore, if moisture variations are not a major factor regarding temporal trends in snowline position, and assuming a lapse rate of −0.6 °C/100 m, the change in temperature (ΔT) from 1986 to 2005 in the Cordillera Huayhuash would range from +0.01 °C to +0.7 °C, equivalent to an average of +0.2 °C/decade. The ΔT estimates are derived from individual maximum and minimum SLA changes in glaciers with rising SLAs from 1986 to 2005 in the Cordillera Huayhuash. When similar analysis is made in regard to the Cordillera Raura, the ΔT from 1986 to 2005 is +0.02 °C to +1.4 °C, equivalent to an average of +0.36 °C/decade. For the Cordillera Huayhuash, the ΔT estimate only included glaciers with rising trends to create an accurate representation of glaciers with a decreasing mass balance. If falling SLAs are included in temperature change calculations, the ΔT range for the two ranges combined is −0.25 °C to +1.4 °C, or an average of 0.58 °C/decade.

Data analyzed by Vuille and Bradley (2000) estimate recent temperature change of +0.09 °C/decade to +0.16 °C/decade in the Andes Mountains derived from regional climate data in between 4000 m a.s.l. and 5000 m a.s.l., providing a fairly accurate base assessment of the temperature change inferred by the rising SLAs in the Cordilleras Huayhuash and Raura during the study period. Their mean ΔT value was +0.11 °C/decade from 1939–1998 with a significant increase to +0.34 °C/decade from 1973–1998 in the Tropical Andes. The linear temperature increase suggested by their data can explain the linear SLA rise in the Cordillera Raura from 1986 to 2005 (Fig. 8). However, changes in the Cordillera Huayhuash's SLAs have been variable throughout the study period and cannot be explained by a linear temperature increase alone.

TCD
4, 1931–1966, 2010

Our temperature reconstructions assume that moisture variations do not contribute to SLA change over the study period from 1986 to 2005 as indicated by Francou et al. (2004) and Kaser and Osmaston (2002). Annual data from Huaraz, Peru located at 9°31′36.91″ S, 77°31′37.35″ W on the western, drier side of the range (slightly to the SW of the main branch of the Cordillera Blanca) support our moisture variation assumptions. Precipitation totals for Huaraz (3090 m a.s.l.) are assumed to represent the same regional precipitation patterns expected in the Cordillera Huayhuash and the Cordillera Raura since Huaraz lies slightly west of the neighboring Cordillera Blanca and similar rate of glacier SLA rise between the Cordilleras Huayhuash and Blanca (e.g. Mark and Seltzer, 2005) in the recent past in these regions suggest comparable precipitation variations. This is the closest weather station with fairly continuous data that may represent weather patterns for the nearby cordilleras. A weak tendency toward increased precipitation has been recorded for this region (Vuille et al., 2003, 2008), suggesting precipitation change is not responsible for negative mass balance measurements.

Despite several data sources suggesting precipitation has minimal impact on SLA change in the Cordilleras Huayhuash and Raura, different climate changes may have occurred in the Cordillera Huayhuash and the Cordillera Raura over the study period from 1986 to 2005. Since reliable, consistent climate data are not available for elevations above the glacial termini, no definite changes in precipitation between the two ranges can be assessed.

The comparison between the average SLAs in the Cordillera Huayhuash and Raura indicates that temperature change is the prominent factor influencing SLA position with precipitation serving as a secondary control. If these assumptions and conclusions are valid, the data suggest that the zero degree isotherm in this region of the central Andes in Peru has increased to approximately 5080 m a.s.l. as indicated by the comparable SLAs for the most recent years of the study. Therefore, the steady SLA rise displayed by the Cordillera Raura can be interpreted as the glacial response to modern temperature increases in that region. The variable patterns exhibited by the Cordillera

TCD
4, 1931–1966, 2010

Huayhuash SLAs during this time period reflect variations in precipitation overlying a more dominant long-term increase in temperature. Although SLA spatial variations in the Cordillera Huayhuash suggest that contributions from hypsometry, humidity, shading, and microclimate affect the SLAs, the overall control determining the general SLA position is temperature change as indicated by the similar SLAs for both ranges since the late 1990's (Fig. 8).

Climate variability controls SLA position throughout the range as well as local characteristics. Microclimate in individual glaciated valleys also plays a crucial role in glacial change as climate response varies between valleys throughout the range. The effects of microclimate can be displayed through SLA variations during El Niño and La Niña cycles. According to Wagnon et al. (2001), referring to the Zongo glacier in the Bolivian Altiplano, a strong negative mass balance should occur in tropical glaciers during El Niño conditions. According to Francou et al. (1995), the Cordillera Huayhuash may experience increased ablation rates from higher air temperatures during El Niño conditions with precipitation differences playing a negligible role if El Niño effects are similar in the Andes of central Peru to those in the Bolivian Altiplano. Despite the strong El Niño documented between 1997 and 1998, SLA changes between 1996 (not El Nino) and 1997 (strong El Nino) do not reflect the strong El Niño conditions of 1997 with a mean SLA rise from 5039 ± 46 m a.s.l. to 5043 ± 25 m a.s.l., respectively. Similarly, there is no obvious lag in El Niño effects represented in the mean SLA in 1999. According to Francou et al. (1995), we should expect to see the largest El Niño effects between February and November in the Ecuadorian Andes resulting in SLA rises from 1997 to 1998. Data from 1997 to 1999 do not reflect any large SLA rises.

The overall increase in the mean SLA is moderated by high interannual variability and several glaciers show no trend with respect to predicted changes from strong El Niño conditions in 1997. In fact, some glaciers had lower SLAs in 1997 compared to 1996, which is contradictory to expected SLA rise related to temperature measurements recorded by Vuille et al. (2008) for the tropical Andes. As recorded by Vuille et al. (2008), 1996 and 1999 were the only years within the past 20 years with

TCD
4, 1931–1966, 2010

temperatures below the long term (1961–1999) average. The deviation from the expected SLA variability may indicate that microclimate conditions are more important to SLA positions than the regional effects such as El Niño conditions.

The tropical impacts are already well known to those who depend on high elevation glaciers for water for consumption, agriculture, and hydroelectric power, because 80% of the water resources on the Pacific side of Peru originate from the snow and ice in the Andes (Coudrain et al., 2005). Overall, the glacial change indicated by the rising SLAs in both the Cordillera Huayhuash and the Cordillera Raura from 1986 to 2005 indicates a temperature increase in tropical regions. If the SLA rises are close to the upper estimate in the Cordillera Raura of +1.4 °C over 20 years, the implications are staggering.

Acknowledgements. We thank NASA for its financial support for this research as well as Lehigh University for the computer infrastructure used for data analysis. Funding for research was provided by the NASA New Investigator Program (Grant NNG04GO95G to Joan Ramage) and was used to support the work and the purchase of NASA/USGS data. We would also like to thank the Global Land Cover Facility (GLCF) at the University of Maryland and EROS Data Center-NASA/USGS for the use of available satellite imagery in such a remote region of the world. We thank Bryan Mark and Joshua Galster for their helpful comments regarding revisions to the paper, Mathias Vuille for providing data prior to publication, and Eloise Kaizar for help with the use of statistics.

References

Andrews, J.: Glacial Systems: An approach to glaciers and their environments, North Scituate, MA, Duxbury Press, 191 pp., 1975.

Bliss, N. B. and Olsen, L. M.: Development of a 30-arc-second digital elevation model of South America, Pecora Thirteen, Human Interactions with the Environment-Perspectives from Space, Sioux Falls, South Dakota, 20–22 August, 1996.

Bookhagen, B. and Strecker, M.: Orographic barriers, high-resolution TRMM rainfall,

TCD

4, 1931–1966, 2010

and relief variations along the eastern Andes, Geophys. Res. Lett., 35, L06403, doi:10.1029/2007GL032011, 2008.
Bradley, R., Vuille, M., Diaz, H., and Vergara, W.: Threats to water supplies in the tropical Andes, Science, 312, 1755–1756, doi:10.1126/science.1128087, 2006.
Chander, G. and Markham, B.: Revised Landsat-5 TM radiometric calibration procedures and postcalibration dynamic ranges, IEEE T. Geosci. Remote, 24, 2674–2677, 2003.
Coudrain, A., Francou, B., Kundzewicz, Z. W.: Glacier shrinkage in the Andes and consequences for water resources, Hydrolog. Sci. J., 50, 925–932 2005.
De Angelis, H., Rau, F., and Skvarca, P.: Snow zonation on Hielo Patagónico Sur, Southern Patagonia, derived from Landsat 5 TM data, Global Planet. Change, 59, 149–158, 2007.
Dornbusch, U.: Current large scale climatic conditions in south Peru and their influence on snowline altitudes, Erdkunde, 52, 41–54, 1998.
Francou, B., Ribstein, P., Semiond, H., Portocarrero, C., and Rodriguez, A.: Balances de glaciares y clima en Bolivia y Peru: impacto de los eventos ENSO, Bulletin de l'Institut Francais d'Etudes Andines, 24, 661–670, 1995.
Francou, B., Vuille, M., Favier, V., and Caceres, B.: New evidence for an ENSO impact on low-latitude glaciers; Antizana 15, Andes of Ecuador, 0 degrees 28′ S, J. Geophys. Res., 109, D18106, doi:10.1029/2003JD004484, 2004.
Kaser, G., Georges, C., and Ames, A.: Modern glacier fluctuations in the Huascaran-Chopicalqui-Massif of the Cordillera Blanca, Peru, Zeitschrift fuer Gletscherkunde und Glazialgeologie, 32, 91–99, 1996.
Kaser, G. and Georges, C.: Changes of the equilibrium-line altitude in the tropical Cordillera Blanca, Peru, 1930–1950, and their spatial variations, Ann. Glaciol., 24, 344–349 1997.
Kaser, G. and Osmaston, H.: Tropical glaciers, Cambridge, Cambridge University Press, 47–207, 2002.
Kaser, G., Juen, I., Georges, C., Gomez, J., and Tamayo, W.: The impact of glaciers on the runoff and the reconstruction of mass balance history from hydrological data in the tropical Cordillera Blanca, Peru, J. Hydrol., 282, 130–144, doi:10.1016/S0022-1694(03)00259-2, 2003.
Klein, A. and Isacks, B.: Alpine glacier geomorphological studies in the central Andes using Landsat Thematic Mapper images, Glacial Geology and Geomorphology, rp01/1998, 1998.
Mark, B., Seltzer, G., Rodbell, D., and Goodman, A.: Rates of deglaciation during the last glaciation and Holocene in the Cordillera Vilcanota-Quelccaya Ice Cap region, Southeastern

TCD
4, 1931–1966, 2010

Peru, Quaternary Res., 57, 287–298, 2002.
Mark, B. G.: Hydrochemical evaluation of changing glacier meltwater contribution to stream discharge: Callejon de Huaylas, Peru, Hydrolog. Sci., 50, 975–987, 2005.
Mark, B. G. and Seltzer, G. O.: Evaluation of recent glacier recession in the Cordillera Blanca, Peru (AD 1962–1999): spatial distribution of mass loss and climatic forcing, Quaternary Sci. Rev., 24, 2265–2280, 2005.
Morales Arnao, C.: Las Cordilleras del Peru, Universidad de San Martin de Porres: Tarea Asociación Gráfica Educativa, 29–165, 2001.
Schwerdtfeger, W.: Climates of Central and South America, World Survey of Climatology, 12, 153–173, 1976.
Vuille, M. and Bradley, R.: Mean annual temperature trends and their vertical structure in the tropical Andes, Geophys. Res. Lett., 27, 3885–3888, 2000.
Vuille, M., Bradley, R., Werner, M., and Keimig, F.: 20th century climate change in the tropical Andes; observations and model results, Climate variability and change in high elevation regions; past, present, and future, Climatic Change, 59, 75–99, 2003.
Vuille, M., Francou, B., Wagnon, P., Juen, I., Kaser, G., Mark, B., and Bradley, R.: Climate change and tropical Andean glaciers: Past, present and future, Earth-Sci. Rev., 89, 79–96, 2008.
Wagnon, P., Ribstein, P., Francou, B., and Sicart, J. E.: Anomalous heat and mass budget of Glacier Zongo, Bolivia, during the 1997/1998 El Niño year, J. Glaciol., 47, 21–28, 2001.
Yanahuanca: Hoja 21-j, Carta Nacional 1:100000 Primera edición, El Instituto Geográfico Nacional, Lima, Peru 1969–1970.

TCD
4, 1931–1966, 2010

Table 1. Landsat 5 and Landsat 7 data were used for SLA measurements. Data were purchased from the United States Geological Society, Eros Data Center (USGS/EDC) or acquired from the Global Land Cover Facility (GLCF) at the University of Maryland. Metadata was extracted from both sources in order to form complete data sets.

Date (mm/dd/yyyy)	Sensor	Source (m)	Resolution (astronomical units)	*d*
22/06/1986	Landsat 5 TM	USGS/EDC	28.5	1.0163
30/12/1989	Landsat 5 TM	GLCF	28.5	0.9833
15/09/1991	Landsat 5 TM	GLCF	28.5	1.0057
24/06/1996	Landsat 5 TM	USGS/EDC	28.5	1.0164
27/06/1997	Landsat 5 TM	USGS/EDC	28.5	1.0165
05/08/1999	Landsat 7 ETM+	USGS/EDC	28.5	N/A
17/06/2002	Landsat 7 ETM+	USGS/EDC	28.5	N/A
06/06/2004	Landsat 7 ETM+	USGS/EDC	28.5	N/A
11/07/2005	Landsat 7 ETM+	USGS/EDC	28.5	N/A

TCD
4, 1931–1966, 2010

Table 2. Band specific data for L_{min} and L_{max} and provided in this Table for spectral radiance calibration. The calibration technique (Eq. 1) is used for all Landsat 5 data.

Band	L_{min}	L_{max}
1	−1.52	152.1
2	−2.84	296.81
3	−1.17	204.3
4	−1.51	206.2
5	−0.37	27.19
7	−0.15	14.38

TCD
4, 1931–1966, 2010

Table 3. Band specific data for solar exoatmospheric irradiance (S) values. These values are used in Eq. 2 to calibrate Landsat 5 data.

Band	S [$Wm^{-2}\,\mu m^{-1}$]
1	1957
2	1826
3	1554
4	1036
5	215
7	80.67

TCD
4, 1931–1966, 2010

Table 4. The mean and standard deviation values for SLAs on each measurable glacier in the Cordillera Huayhuash were extracted from an ASTER DEM. The mean SLA for the range, displayed in the bottom right, is the average of the individual glacier's means for each year. The standard deviation for the average SLA is the average of the individual glacier's standard deviations.

	Jahuacocha (A)		Mitococha (B)		Chaclan (C)		Carhuacocha (D)		Gangrajanca (E)		Quesillococha (F)		Azulcocha (G)	
Year	Mean (m)	Standard Deviation (m)	Mean (m)	Standard Deviation (m)	Mean (m)	Standard Deviation (m)	Mean (m)	Standard Deviation (m)	Mean (m)	Standard Deviation (m)	Mean (m)	Standard Deviation (m)	Mean (m)	Standard Deviation (m)
1986	5272	117	5009	71	4998	57	5132	41	5160	18	4875	40	5149	0
1989	5124	94	5017	50	4927	57	5095	28	5118	30	4880	8	5088	14
1991	5265	95	5007	42	NA	NA	NA	NA	NA	NA	4823	31	NA	NA
1996	5296	138	4992	44	4917	33	5059	23	5120	38	4923	22	5093	14
1997	5200	100	4996	40	4947	48	5071	30	5110	26	4876	25	5094	36
1999	5237	137	5023	42	4938	53	5069	39	5110	43	4876	25	5023	5
2002	5271	128	5055	28	4931	87	5074	34	NA	NA	4979	32	5002	41
2004	5275	112	NA	NA	NA	NA	5092	40	5103	28	5007	23	NA	NA
2005	5291	117	5071	29	4971	21	5111	31	5121	28	4991	40	5109	27
Mean	5248	39	5021	16	4947	21	5090	12	5123	14	4914	10	5080	9

	Carnicero (H)		Barrosacocha (I)		Jurau (J)		Sarapococha (K)		Caramarca (L)		Rasac (M)		Mean SLA	
Year	Mean (m)	Standard Deviation (m)	Mean (m)	Standard Deviation (m)	Mean (m)	Standard Deviation (m)	Mean (m)	Standard Deviation (m)	Mean (m)	Standard Deviation (m)	Mean (m)	Standard Deviation (m)	Mean (m)	Standard Deviation (m)
1986	5030	70	NA	NA	4929	271	NA	NA	NA	NA	NA	NA	5062	36
1989	4992	33	5035	28	4938	194	5147	98	5010	38	NA	NA	5031	25
1991	NA	NA	NA	NA	4897	238	5051	56	NA	NA	NA	NA	5008	54
1996	NA	NA	4992	25	4928	381	5074	86	NA	NA	NA	NA	5039	46
1997	5104	43	5011	18	4946	178	5107	94	5121	130	5394	80	5043	25
1999	NA	NA	NA	NA	4913	177	5118	108	NA	NA	NA	NA	5034	29
2002	5050	16	4920	18	4945	151	5140	109	NA	NA	5474	44	5037	25
2004	5087	9	5041	5	4908	295	NA	NA	NA	NA	NA	NA	5074	46
2005	5109	27	5038	25	4941	320	5193	92	NA	NA	NA	NA	5086	35
Mean	5062	16	5006	9	4927	85	5119	43	5065	68	5434	46	5046	12

TCD
4, 1931–1966, 2010

Table 5. Mean and standard deviation values for all measurable glaciers in the Cordillera Raura and the mean SLA for the range.

	Luychos (N)		Huascacocha (O)		Jaico (P)		Niñococha (Q)		Putusay (R)		Checchi (S)		Yuracocha (T)	
Year	Mean (m)	Standard Deviation (m)	Mean (m)	Standard Deviation (m)	Mean (m)	Standard Deviation (m)	Mean (m)	Standard Deviation (m)	Mean (m)	Standard Deviation (m)	Mean (m)	Standard Deviation (m)	Mean (m)	Standard Deviation (m)
1986	4987	21	4958	36	4991	36	5043	22	5027	18	4834	23	4870	7
1989	5019	36	4984	19	5015	68	5048	15	5076	34	5010	17	4873	4
1997	NA	NA	5036	13	4983	62	5081	7	5069	30	4996	30	5083	37
1999	5010	20	4959	8	4979	60	5065	13	5094	12	4989	27	5106	29
2002	5004	24	4985	9	4994	60	5062	13	5093	18	5009	16	5107	30
2005	NA	NA	NA	NA	NA	NA	NA	NA	NA	NA	NA	NA	5095	43
Mean	5005	13	4984	9	4992	26	5060	7	5072	11	4968	10	5022	12
	Agopampa (U)		Viconga (V)		Aguascocha (W)		Carcamachay (X)		Caballeros (Y)		Mancaneota (Z)		Pichuycocha (AA)	
Year	Mean (m)	Standard Deviation (m)	Mean (m)	Standard Deviation (m)	Mean (m)	Standard Deviation (m)	Mean (m)	Standard Deviation (m)	Mean (m)	Standard Deviation (m)	Mean (m)	Standard Deviation (m)	Mean (m)	Standard Deviation (m)
1986	NA	NA	4743	5	4853	24	4763	19	5135	6	5014	32	5117	31
1989	NA	NA	4799	8	4921	65	4800	15	5130	12	5008	15	5111	20
1997	5088	64	4840	25	4913	55	4911	22	NA	NA	5151	23	5173	71
1999	5112	88	4916	7	5038	23	4952	30	5132	1	5123	23	5188	54
2002	5180	38	4929	16	NA	NA	4948	42	5135	6	5133	28	5196	60
2005	5154	25	4991	7	NA	NA	5041	46	NA	NA	NA	NA	NA	NA
Mean	5134	30	4870	5	4931	23	4903	13	5133	3	5086	11	5157	23
	Santa Rosa (BB)		Condorsenja (CC)		Yanco (DD)		Caballococha (EE)		Mean SLA					
Year	Mean (m)	Standard Deviation (m)	Mean (m)	Standard Deviation (m)	Mean (m)	Standard Deviation (m)	Mean (m)	Standard Deviation (m)	Mean (m)	Standard Deviation (m)				
1986	4985	57	5067	15	4911	30	4802	26	4947	7				
1989	4942	29	5076	10	4908	17	4875	41	4972	7				
1997	4963	68	5074	6	4974	40	4895	26	5014	10				
1999	5027	31	5076	1	4939	14	4880	33	5032	8				
2002	5063	42	5077	0	4938	15	4898	30	5044	8				
2005	NA	NA	NA	NA	NA	NA	NA	NA	5070	17				
Mean	4996	21	5074	4	4934	11	4870	14	5013	4				

TCD
4, 1931–1966, 2010

Table 6. Summary of glacier mean SLA, standard deviation, ELA change, and linear trend data.

Glacier	Mean (m a.s.l.)	SD (m)	SLA Change 1986–2005[a]	Linear Trend	R^2 *
Azulcocha (G)	5080	9.2	−40	−4.0	0.29
Barrosacocha (I)	5006	8.7	2.4	−8.2	**0.86**
Caramarca (L)	5066	67.7	**111 (+)**	13.9	**1**
Carhuacocha (D)	5090	11.9	−21	−1.2	0.12
Carnicero (H)	5062	15.9	**79 (+)**	4.3	**0.57**
Chaclan (C)	4947	20.6	−26.2	−1.0	0.06
Gangrajanca (E)	5123	14.5	**−38.4 (+)**	−1.8	0.49
Jahuacocha (A)	5248	38.8	19	3.3	0.17
Jurau (J)	4927	85.2	12	0.32	0.02
Mitococha (B)	5021	15.9	**62.2 (+)**	2.9	0.45
Quesillococha (F)	4914	9.6	**116 (+)**	7.6	**0.64**
Rasac (M)	5434	45.7	**79.2 (+)**	15.8	**1**
Sarapococha (K)	5119	42.5	−7.5	4.7	0.32
Agopampa (U)	5134	29.6	**72.2 (+)**	9.6	**0.67**
Aguascocha(W)	4932	22.8	**185.6 (+)**	9.9	**0.64**
Caballeros(Y)	5133	3.0	−1.8	0.02	0.006
Caballococha (EE)	4870	14.1	**95.1 (+)**	4.7	**0.66**
Carcamachay (X)	4903	12.7	**278.9 (+)**	13.7	**0.97**
Checchi (S)	4968	10.5	**151.3 (+)**	7.4	0.45
Condorsenja (CC)	5074	3.8	**7.7 (+)**	0.43	**0.54**
Huascacocha (O)	4984	9.0	**25 (+)**	1.4	0.084
Jaico (P)	4992	26.0	5.6	−1.0	0.23
Luychos (N)	5005	13.1	**17.2 (+)**	0.56	0.1
Mancaneota (Z)	5086	11.1	**135.2 (+)**	9.2	**0.84**
Ninococha (Q)	5060	6.7	2.6	1.7	**0.55**
Pichuycocha (AA)	5157	22.7	**75.7 (+)**	5.7	**0.95**
Putusay (R)	5072	10.7	**65.5 (+)**	3.3	**0.67**
Santa Rosa (BB)	4996	21.4	**81.1 (+)**	5.1	**0.51**
Viconga (V)	4870	5.4	**248.8 (+)**	12.1	**0.94**
Yanco (DD)	4934	11.4	8	2.6	0.45
Yuracocha (T)	5022	11.8	**235.9 (+)**	14.7	**0.86**

Note: Glacier names are based on major lakes in the valley or nearby peaks. Names do not necessarily reflect official geographic names. Refer to Fig. 2 for approximate locations. Annual SLAs are reported in Tables 4 and 5 and Fig. 4.
[a] SLA change that is significant at the 95% confidence level is in bold and has a (+) behind the value.
*R^2 values are bold if they exceed 0.5.

TCD
4, 1931–1966, 2010

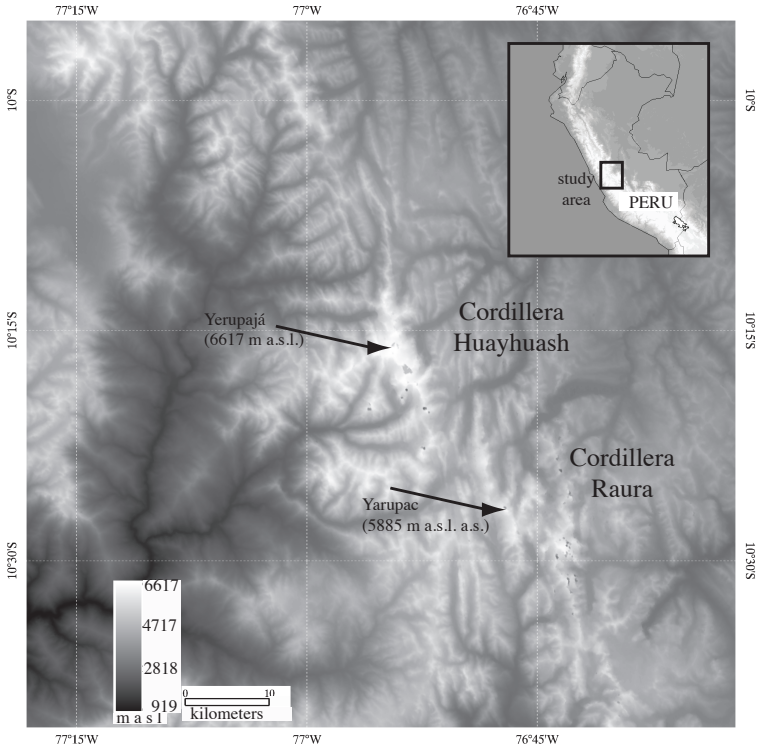

Fig. 1. The Advanced Spaceborne Thermal Emission and Reflection Radiometer (ASTER) DEM of the Cordilleras Huayhuash and Raura was used for SLA measurements due to its high, uniform resolution (15-m). DEM elevations range from 3275 m to 5715 m, although the highest true elevation occurs at 6617 m. Although the ASTER DEM provides inaccurate elevations in the highest relief areas, its elevations were determined to be reliable up to approximately 5600 m through comparison with the SRTM DEM and topographic maps. The inset map of Peru shows the general location of the cordilleras.

TCD
4, 1931–1966, 2010

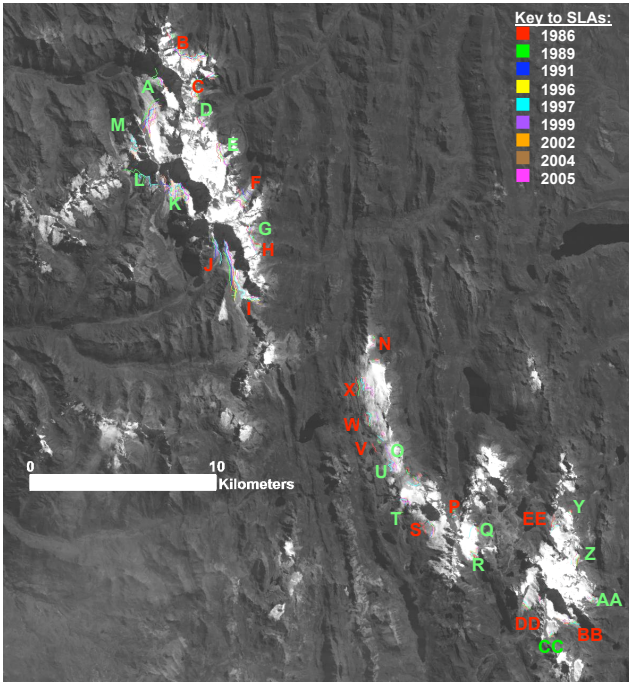

Fig. 2. Snowlines, overlaid on the 27 June, 1997 Landsat 5, Band 3 (red; 0.66 µm) base image. For all gray scale Landsat images, snow is white, ice is light gray, rock and vegetation are dark gray, and water is black. The key indicates the color for each year's snowline, representing the annual SLA. Green labels represent glaciers with above average SLAs and those with red labels represent glaciers with below average SLAs. Glaciers are labeled as follows: Jahuacocha (A), Mitococha (B), Chaclan (C), Carhuacocha (D), Gangrajanca (E), Quesillococha (F), Azulcocha (G), Carnicero (H), Barrosacocha (I), Jurau (J), Sarapococha (K), Caramarca (L), Rasac (M), Luychos (N), Huascacocha (O), Jaico (P), Niñococha (Q), Putusay (R), Checchi (S), Yuracocha (T), Agopampa (U), Viconga (V). Aguascocha (W), Carcamachay (X), Caballeros (Y), Mancaneota (Z), Pichuycocha (AA), Santa Rosa (BB), Condorsenja (CC), Yanco (DD), Caballococha (EE).

TCD
4, 1931–1966, 2010

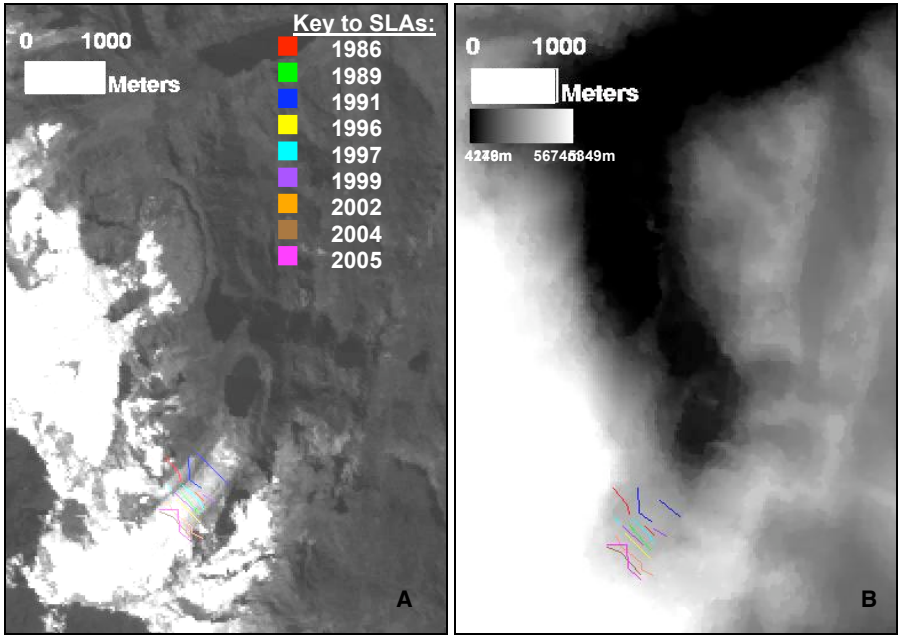

Fig. 3. Snowlines for the Quesillococha glacier (F on Fig. 2) are overlaid on **(A)** the 1997 Landsat base image and **(B)** the gray scale ASTER DEM. The key in A applies to both images. Though located in the same valley as the Gangrajanca glacier, the Quesillococha glacier displays a drastic snowline rise from 1986 to 2005 quite different from the Gangrajanca SLA trend (not shown, Table 4). The snowlines were overlaid on the DEM to quantify the rise from 1986–2005.

TCD
4, 1931–1966, 2010

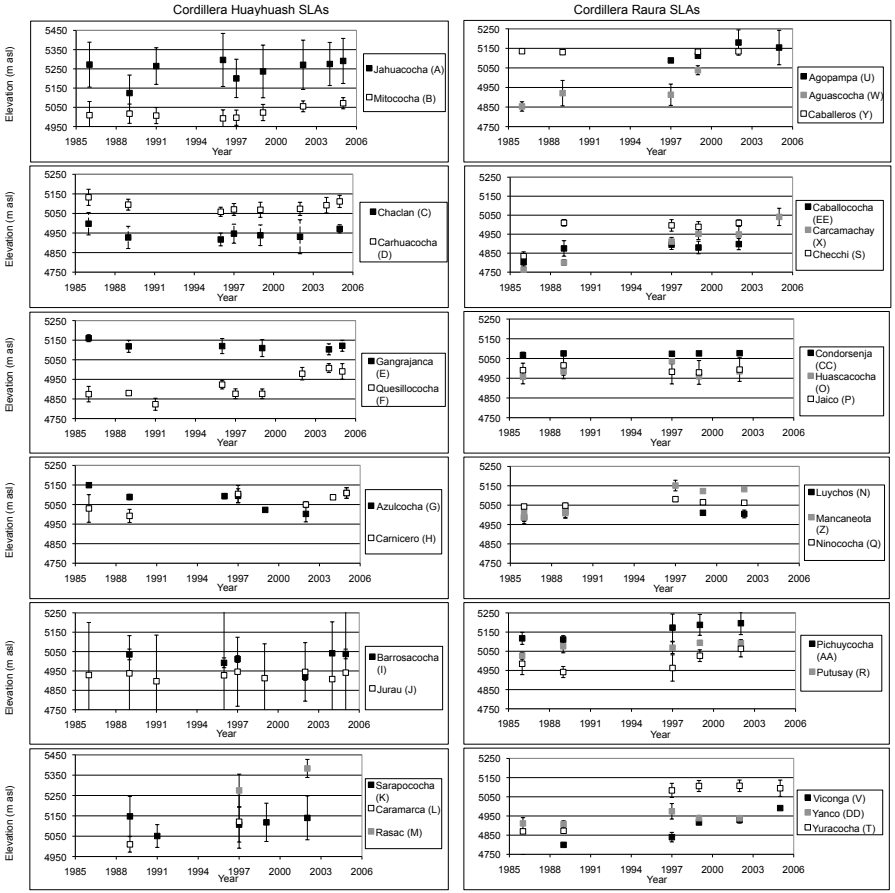

Fig. 4. Mean SLAs for each glacier for both the Cordillera Huayhuash and Cordillera Raura. The error bars represent ± one standard deviation from the mean. All Y-axes have the same range (500 m) although the altitudes vary. See Tables 4 and 5 for the values for each glacier.

TCD
4, 1931–1966, 2010

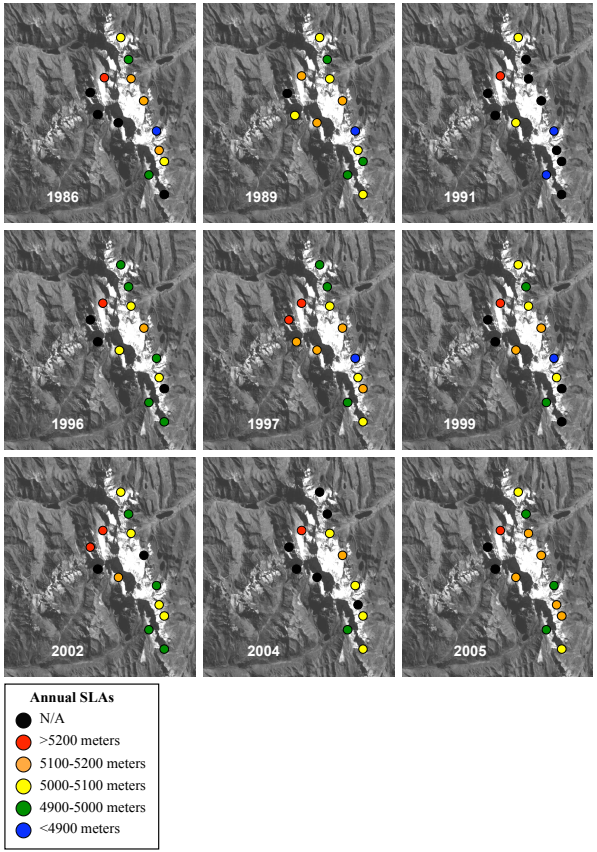

Fig. 5. Time series of the Cordillera Huayhuash SLAs from 1986–2005. Data gaps represented by black circles are primarily attributed to shadow or poor snow-ice differentiation. As shown in the time series, the snowlines on the western side of the ridge tend to have higher SLAs than those on the eastern side. Little annual change can be distinguished in several images due to large elevation categories.

TCD
4, 1931–1966, 2010

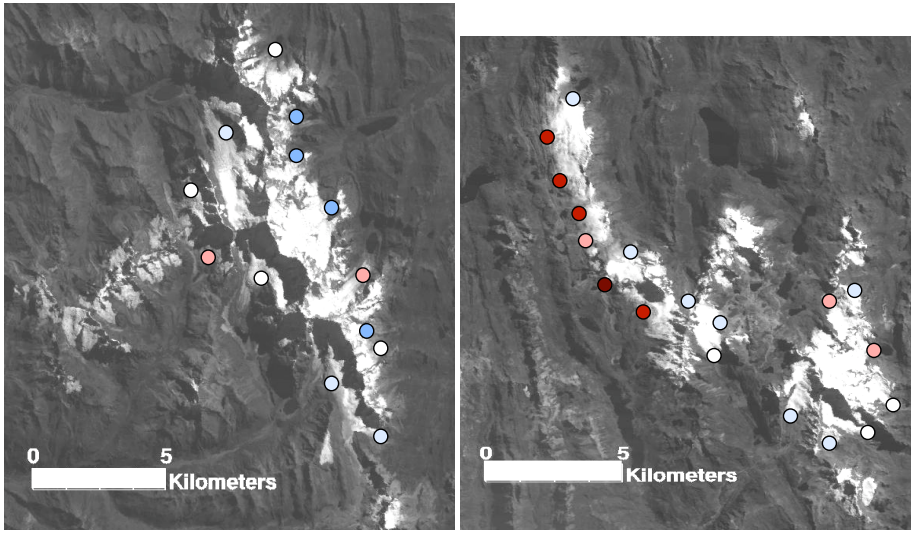

Fig. 6. SLA change from 1986 to 2005 in the Cordillera Huayhuash (A) and the Cordillera Raura (B). The ΔSLA values for individual glaciers are shown as colored circles. Dark red circles indicate the largest SLA rise and darker blue circles indicate a slight SLA fall over the 20 year study period. The Cordillera Raura SLAs rose significantly more than the Cordillera Huayhuash SLAs over the same duration with the most drastic rise along the western edge of the Cordillera Raura's ridge.

TCD
4, 1931–1966, 2010

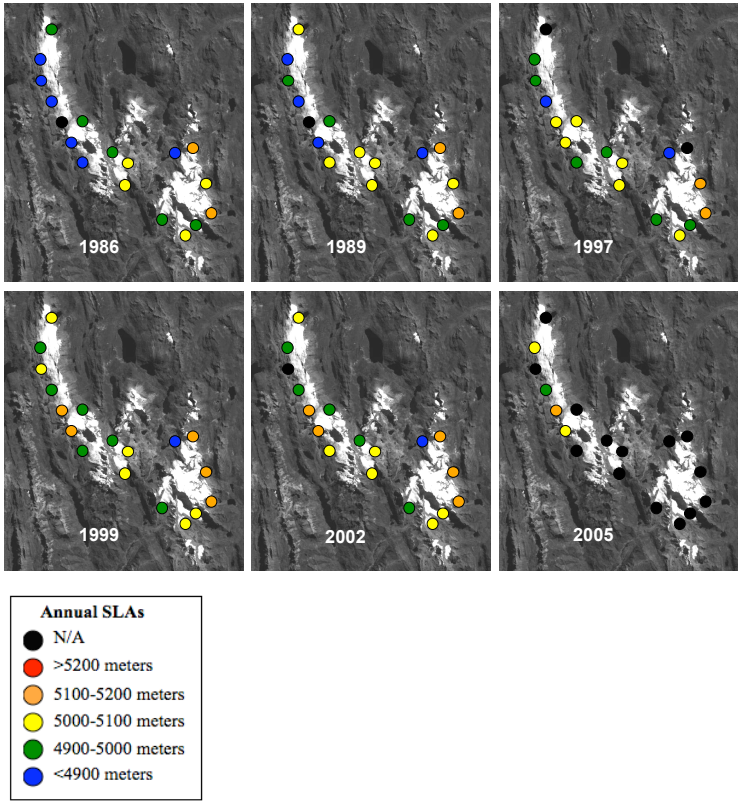

Fig. 7. Time series of the Cordillera Raura SLAs from 1986–2005. Data gaps represented by black circles are due to shadow or poor snow-ice differentiation. In contrast with the Cordillera Huayhuash, the SLAs on the western side of the ridge tend to have lower SLAs than those on the eastern side. Little annual change can be distinguished in several images due to large elevation categories.

TCD
4, 1931–1966, 2010

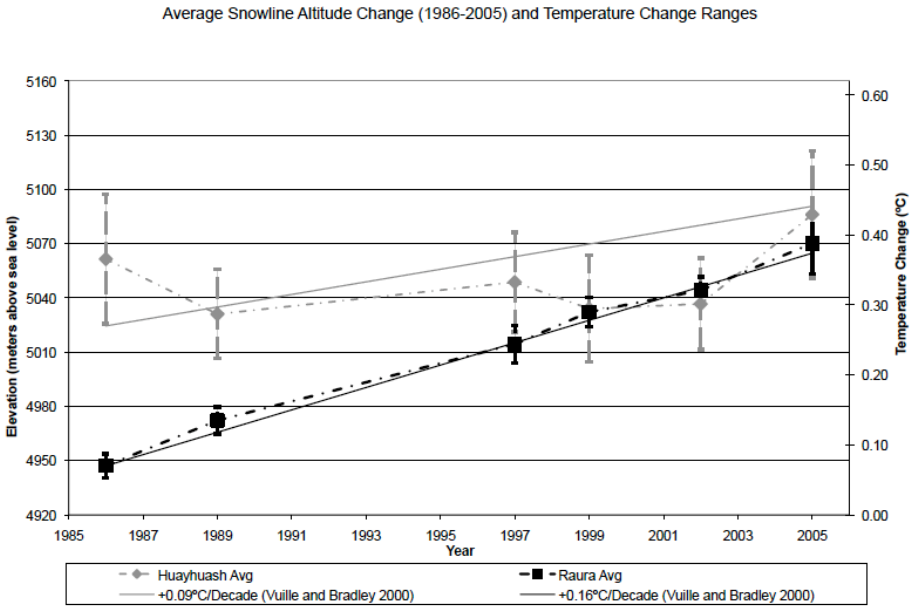

Fig. 8. Comparison of the mean SLAs calculated for the Cordillera Huayhuash and Cordillera Raura. The mean SLAs are calculated for each range using the mean of all available SLAs for each year. The standard deviations shown on the plot are calculated using the square root of the sum of the variances of the individual SLAs for each year.

TCD
4, 1931–1966, 2010